Constraint-combined Force / Position Hybrid Control Method for Continuous Shape-grinding

Guanghua Chen, Mamoru Minami, Geng Wang, Akira Yanou, Mingcong Deng
Graduate School of Natural Science and Technology, Okayama University
Tsushimanaka3-1-1 , Okayama, JAPAN
Email: {Guanghua Chen, minami, owg_cyo, yanou, deng}@suri.sys.okayama-u.ac.jp

***Abstract*—Based on the analysis of the interaction between a manipulator's hand and a working object, a model representing the constrained dynamics of the robot is first discussed. The constraint forces are expressed by an algebraic function of states, input generalized forces, and constraint condition, and then direct position / force controller without force sensor is proposed based on the algebraic relation. To give the grinding system the ability to adapt to any object shape being changed by the grinding, we added estimating function of the constraint condition in real time for the adaptive position / force control, which is indispensable for our method instead of not using force sensor. Evaluations through continuous shape-grinding experiment by fitting the changing constraint surface with spline functions, indicates that reliable position / force control and shape-grinding work can be achieved by this proposed controller.**

I. Introduction

Many researches have discussed on the force control of robots for contacting tasks. Most force control strategies are to use force sensors [1]-[3] to obtain force information, where the reliability and accuracy are limited since the work-sites of the robot are filled with noise and thermal disturbances, reducing the sensor's reliability. On top of this, force sensors could lead to the falling of the structure stiffness of manipulators, which is one of the most essential defects for manipulators executing grinding tasks. To solve these problems, some approaches using no force sensor have been presented [4],[5]. To ensure the stabilities of the constrained motion, those force and position control methods have utilized Lyapunov's stability analysis under the inverse dynamic compensation [6]-[8]. Their force control strategies have been explained intelligibly in books [9],[10] and recently interaction control for six-degree-of-freedom tasks has been compiled in a book [11].

Those former classical robot controlling approaches can be classified into two broad categories [8]: impedance control and hybrid (force/position) control. In impedance control, a prescribed dynamic relation is sought to be maintained between the robot end-effector's force exerting to a object constraining the end-effector and position displacement toward the direction vertical to the object's surface [12]. In hybrid control, the end-effector's force is explicitly controlled in selected directions and the end-effector's position is controlled in the remaining (complementary) directions [1].

The hybrid control approaches can be further classified into three main categories: 1) explicit (model based) hybrid control of rigid robots in elastic contact with a compliant environment, e.g., [13],[14], in which the end-effector force is controlled by directly commanding the joint torques of the robot based on the sensed force error; 2) implicit (position/velocity based) hybrid control of rigid robots in elastic contact with a compliant environment, e.g., [15], in which the end-effector force is controlled indirectly by modifying the reference trajectory given into an inner loop joint position/velocity controller based on the sensed force error; and 3) explicit (model based) hybrid control of rigid robots in hard contact with a rigid environment, e.g., [1],[3].

According to these classified categories, our force/position control approach named as Constraint-Combined Control, which will be detailly introduced later should be classified into category 3). In all the former force/position controlling methods of hybrid control of category 1) and 2), the contact surface's compliant characteristics must be properly taken into account since it will affect force control procedure. As a result, when contact constraint force is analyzed, process the end-effector contacting with constraint surface is being expressed as a motion equation with spring model, which is a differential function with time-varying.

However, the work-piece being ground by our grinding robot in this paper is iron, of which the spring constant is so huge that we can ignore the deformation of the work-piece caused by the contacting force with robot's end-effector. So the contact process of the grinder can be just thought as non-dynamical process but a kinematical one, there is no motion occurred in vertical direction against contacting surface. Therefore, in our research we don't use the time-differential motion equation to analyze contacting vertical process to the work-piece, on the contrary, we consider an algebraic equation as the constraint condition to analyze this contact vertical force. Constraint-combined Force Controller based on this algebraic equation has the ability to achieve the force control without time delay, moreover, force error will not be affected by the dynamical motion along to the surface in horizonal direction. In explicit hybrid control field in category 3), some former researches have noticed this "just an immediate contact result but no motion occurred" problem and try to solve it by using force or torque sensor. But since force or torque sensor is so costly, we consider a new force / position control method without using sensors. Therefore, with these differences from those former force control methods, we can announce that Constraint-Combined force / position control method without using sensors introduced in this paper can be thought to be essentially different from methods proposed so far.

Eq.(1), which has been pointed out by Hemami [16] in the analysis of biped walking robot, denotes also algebraic relation between the input torque $\boldsymbol{\tau}$ of the robot and exerting force to the working object F_n, when robot's end-effecter being in touch with a surface in 3-D space:

$$F_n = a(\boldsymbol{x}_1, \boldsymbol{x}_2) - \boldsymbol{A}(\boldsymbol{x}_1)\boldsymbol{\tau}, \tag{1}$$

where, $\boldsymbol{x}_1$ and $\boldsymbol{x}_2$ are state variables. $a(\boldsymbol{x}_1, \boldsymbol{x}_2)$ and $\boldsymbol{A}(\boldsymbol{x}_1)$ are scalar function and vector one defined in following section.

A strategy to control force and position proposed in this paper is also based on Eq.(1). Contrarily to Peng's Method [7] to use Eq.(1) as a force sensor, we used the equation for calculating $\boldsymbol{\tau}$ to achieve a desired exerting force F_{nd}. Actually, the strategy is based on two facts of Eq.(1) that have been ignored for a long time. The first fact is that the force transmission process is an immediately process being stated clearly by Eq.(1) providing that the manipulator's structure is rigid. Contrarily, the occurrence of velocity and position is a time-consuming process. By using this algebraic relation, it's possible to control the exerting force to the desired one without time lag. Another important fact is the input generalized forces have some redundancy against the constrained generalized forces in the constrained motion. Based on the above analyses, we had confirmed our force / position control method can realize the grinding task through real grinding robot [17], [18].

In this paper, position and force control performances of our new controller [17] are confirmed by grinding experiments, especially on the view point that the force control space and the position control space are divided into orthogonal spaces being complement each other, that is, force space is defined by range space of $\boldsymbol{A}$ and the other is null space of $\boldsymbol{A}$, $(\boldsymbol{I} - \boldsymbol{A}^{+}\boldsymbol{A})$.

The problem to be solved in our approach is that the mathematical expression of algebraic constraint condition should be defined in the controller instead of the merit of not using force sensor. Grinding task requires on-line estimation of changing constraint condition since the grinding is the action to change the constraint condition in nature. In this paper, we estimate the object's surface using the grinder as a touch sensor. In order to give the system the ability to grind any working object into any shape, we focus on how to update the constraint condition in real time, obtaining the result that spline function is best for on-line shape estimation. Based on the above preparation we constructed a continuous shape-grinding experiment to evaluate the proposed shape-grinding system, resulting in having proven the validity of our system to have the performance to adapt for grinding to desired-shape without force sensor.

II. Analysis of Grinding Task

Generally speaking, the grinding power is related to the metal removal rate(weight of metal being removed within unit time), which is determined by the depth of cut, the width of cut, the linear velocity of the grinding wheel, the feed rate and so on. There are many empirical formulae available for the determination of grinding power, and the desired force

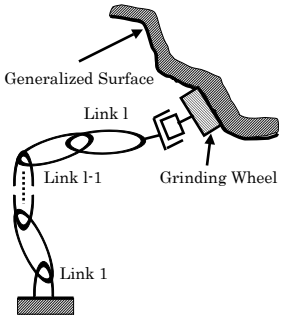

Fig. 1. A Grinding Robot

trajectory can then be planned according to the power. The normal grinding force F_n is exerted in the perpendicular direction of the surface. It is a significant factor that affects ground accuracy and surface roughness of workpiece. The value of it is also related to the grinding power or directly to the tangential grinding force as

$$F_t = \mathrm{K_t} F_n, \tag{2}$$

where, $\mathrm{K_t}$ is an empirical coefficient, F_t is the tangential grinding force. The axial grinding force F_s is proportional with the feed rate, and is much smaller than the former force.

Eq. (2) is based on the situation that position of the grinding cutter is controlled like currently used machining center. But when a robot is used for the grinding task, the exerting force to the object and the position of the grinding cutter should be controlled simultaneously. The F_n is generally determined by the constrained situation, and it is not suitable to apply Eq. (2) to grinding motion by the robots.

III. Modelling

A. Constrained Dynamic Systems

Hemami and Wyman have addressed the issue of control of a moving robot according to constraint condition and examined the problem of the control of the biped locomotion constrained in the frontal plane. Their purpose was to control the position coordinates of the biped locomotion rather than generalized forces of constrained dynamic equation involved the item of generalized forces of constraints. And the constrained force is used as a determining condition to change the dynamic model from constrained motion to free motion of the legs. In this paper, the grinding manipulator shown in Fig. 1, whose end-point is in contact with the constrained surface, is modelled according Eq. (3) with Lagrangian equations of motion in term of the constraint forces, refering to what Hemami and Arimoto have done:

$$\frac{d}{dt}\left(\frac{\partial L}{\partial \dot{\boldsymbol{q}}}\right) - \left(\frac{\partial L}{\partial \boldsymbol{q}}\right) = \boldsymbol{\tau} + \boldsymbol{J_c}^{T}(\boldsymbol{q})F_n - \boldsymbol{J_r}^{T}(\boldsymbol{q})F_t, \tag{3}$$

where, $\boldsymbol{J_c}$ and $\boldsymbol{J_r}$ satisfy,

$$\boldsymbol{J_c} = \frac{\partial C}{\partial \boldsymbol{q}} / \parallel \frac{\partial C}{\partial \boldsymbol{r}} \parallel = \frac{\partial C}{\partial \boldsymbol{r}} \tilde{\boldsymbol{J}}_r \,/\, \parallel \frac{\partial C}{\partial \boldsymbol{r}} \parallel,$$

$$\tilde{\boldsymbol{J}}_r = \frac{\partial \boldsymbol{r}}{\partial \boldsymbol{q}}, \qquad \boldsymbol{J}_r^{T} = \tilde{\boldsymbol{J}}_r^{\,T} \dot{\boldsymbol{r}} / \parallel \dot{\boldsymbol{r}} \parallel,$$

$\boldsymbol{r}$ is the l position vector of the hand and can be expressed as a kinematic equation ,

$$\boldsymbol{r} = \boldsymbol{r}(\boldsymbol{q}). \tag{4}$$

L is the Lagrangian function, $\boldsymbol{q}$ is $l(\geq 2)$ generalized coordinates, $\boldsymbol{\tau}$ is l inputs. The discussing robot system does not have kinematical redundancy. C is a scalar function of the constraint, and is expressed as an equation of constraints

$$C(\boldsymbol{r}(\boldsymbol{q})) = 0, \tag{5}$$

F_n is the constrained force associated with C and F_t is the tangential disturbance force.

Eq. (3) can be derived to be

$$\boldsymbol{M}(\boldsymbol{q})\ddot{\boldsymbol{q}}+\boldsymbol{H}(\boldsymbol{q},\dot{\boldsymbol{q}})+\boldsymbol{G}(\boldsymbol{q})=\boldsymbol{\tau}+\boldsymbol{J}_c^T(\boldsymbol{q})F_n-\boldsymbol{J}_r^T(\boldsymbol{q})F_t, \tag{6}$$

where $\boldsymbol{M}$ is an $l \times l$ matrix, $\boldsymbol{H}$ and $\boldsymbol{G}$ are l vectors. The state variable $\boldsymbol{x}$ is constructed by adjoining $\boldsymbol{q}$ and $\dot{\boldsymbol{q}}$: $\boldsymbol{x} = (\boldsymbol{x}_1^T, \boldsymbol{x}_2^T)^T$=$(\boldsymbol{q}^T, \dot{\boldsymbol{q}}^T)^T$. The state-space equation of the system are

$$\begin{aligned} \dot{\boldsymbol{x}}_1 &= \boldsymbol{x}_2, \\ \dot{\boldsymbol{x}}_2 &= -\boldsymbol{M}^{-1}(\boldsymbol{H}(\boldsymbol{x}_1,\boldsymbol{x}_2)+\boldsymbol{G}(\boldsymbol{x}_1)) \\ &\quad +\boldsymbol{M}^{-1}(\boldsymbol{\tau}+\boldsymbol{J}_c^T(\boldsymbol{x}_1)F_n-\boldsymbol{J}_r^T\boldsymbol{x}_1)F_t), \end{aligned} \tag{7}$$

or in the compact form

$$\dot{\boldsymbol{x}} = \boldsymbol{F}(\boldsymbol{x},\boldsymbol{\tau},F_n,F_t), \tag{8}$$

Using the inverted form of combination from Eq. (5) and Eq.(8) (this part had been detailedly introduced in [19] by us), F_n can be expressed as

$$F_n = F_n(\boldsymbol{x},\boldsymbol{\tau},F_t), \tag{9}$$

or in a more detailed form

$$\begin{aligned} F_n &= [(\frac{\partial C}{\partial \boldsymbol{q}})\boldsymbol{M}^{-1}(\frac{\partial C}{\partial \boldsymbol{q}})^T]^{-1} \parallel \frac{\partial C}{\partial \boldsymbol{r}} \parallel \\ &\{-[\frac{\partial}{\partial \boldsymbol{q}}(\frac{\partial C}{\partial \boldsymbol{q}})\dot{\boldsymbol{q}}]\dot{\boldsymbol{q}}+(\frac{\partial C}{\partial \boldsymbol{q}})\boldsymbol{M}^{-1}(\boldsymbol{H}(\boldsymbol{q},\dot{\boldsymbol{q}})+\boldsymbol{G}(\boldsymbol{q})+{\boldsymbol{J}_{\boldsymbol{r}}}^T F_t)\} \\ &\quad -[(\frac{\partial C}{\partial \boldsymbol{q}})\boldsymbol{M}^{-1}(\frac{\partial C}{\partial \boldsymbol{q}})^T]^{-1} \parallel \frac{\partial C}{\partial \boldsymbol{r}} \parallel \{(\frac{\partial C}{\partial \boldsymbol{q}})\boldsymbol{M}^{-1}\}\boldsymbol{\tau} \\ &\quad \triangleq a(\boldsymbol{x}_1,\boldsymbol{x}_2)+\boldsymbol{A}(\boldsymbol{x}_1)\boldsymbol{J}_r^T F_t-\boldsymbol{A}(\boldsymbol{x}_1)\boldsymbol{\tau}, \end{aligned} \tag{10}$$

where, $a(\boldsymbol{x}_1,\boldsymbol{x}_2)$ is a scalar representing the first term in the expression of F_n, and $\boldsymbol{A}(\boldsymbol{x}_1)$ is an l vector to represent the coefficient vector of $\boldsymbol{\tau}$ in the same expression. Eq. (8) and Eq. (9) compose a constrained system that can be controlled, if $F_n = 0$, describing the unconstrained motion of the system.

Substituting Eq. (10) into Eq. (7), the state equation of the system including the constrained force (as $F_n > 0$) can be rewritten as

$$\begin{aligned} \dot{\boldsymbol{x}}_1 &= \boldsymbol{x}_2, \\ \dot{\boldsymbol{x}}_2 &= -\boldsymbol{M}^{-1}[\boldsymbol{H}(\boldsymbol{x}_1,\boldsymbol{x}_2)+\boldsymbol{G}(\boldsymbol{x}_1)-\boldsymbol{J}_c^T(\boldsymbol{x}_1)a(\boldsymbol{x}_1,\boldsymbol{x}_2)] \\ &\quad +\boldsymbol{M}^{-1}[(\boldsymbol{I}-\boldsymbol{J}_c^T\boldsymbol{A})\boldsymbol{\tau}+(\boldsymbol{J}_c^T\boldsymbol{A}-\boldsymbol{I})\boldsymbol{J}_r^T F_t], \end{aligned} \tag{11}$$

Solutions of these dynamic equation always satisfy the constrained condition Eq. (5).

B. Shape grinding

In the past, we did the grinding experiment one time when working surface is flat to verify the feasibility of this force-sensorless position/force control method [17]. At that time, we just could do flat grinding work in experiment which is shown in Fig. 4. And then we did the continuous shape grinding simulations to try to extend the grinding ability of our grinding robot [19]. Now in this paper, the continuous shape grinding experiment which has been done by the proposed force sensorless position/force control method will be introduced.

To make the grinding task to be different from the former flat grinding experiment, we want to grind the work-piece into the one with different kinds of shapes, for example, grinding the flat surface into a curved one, just like Fig. 3. In Fig. 3, we can find that the desired working surface is prescribed (it can be decided by us.), which means the desired constrained condition C^d is known, so

$$C^d = y - f^d(x) = 0 \tag{12}$$

But the constrained condition $C^{(j)}$ $(j = 1, 2, \cdots, d-1)$ changed by the previous grinding which is in the Dynamic System of Fig. 2 is hard to defined as an initial condition. So we define

$$C^{(j)} = y - f^{(j)}(x) = 0 \tag{13}$$

where, y is the y position of manipulator's end-effector in the coordinates Σw depicted in Fig. 3 and we assume $C^{(1)}$ is known, that is to say, $f^{(1)}(x)$ is initially defined. $f^{(j)}(x)$ is the working surface remained by i-th grinding. And $f^{(j)}(x)$ is a function passing through all points, $(x_1,\ f^{(j)}(x_1))$, $(x_2,\ f^{(j)}(x_2))$, $\cdots$, $(x_p,\ f^{(j)}(x_p))$, these observed points representing the (j)-th constraint condition obtained from the grinding tip position since we proposed previously the grinding tip used for the touching sensor of ground new surface. Here we assume $f^{(j)}(x)$ could be represented by a polynomial of $(p-1)$-th order of x. Given the above p points, we can easily decide the parameters of polynomial function $y = f^{(j)}(x)$. If the current constrained condition can be got successfully, which means the current working surface $f^{(j)}(x)$ can be detected correctly, the distance from the current working surface to the desired working surface

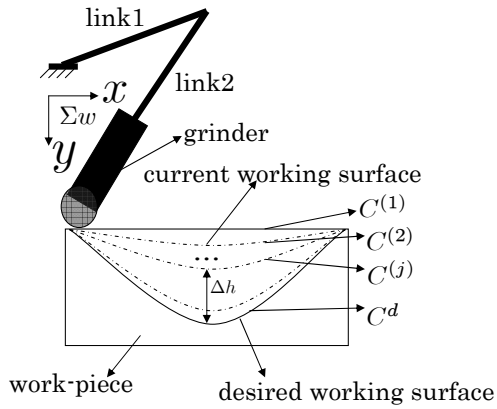

Fig. 3. The model of shape grinding

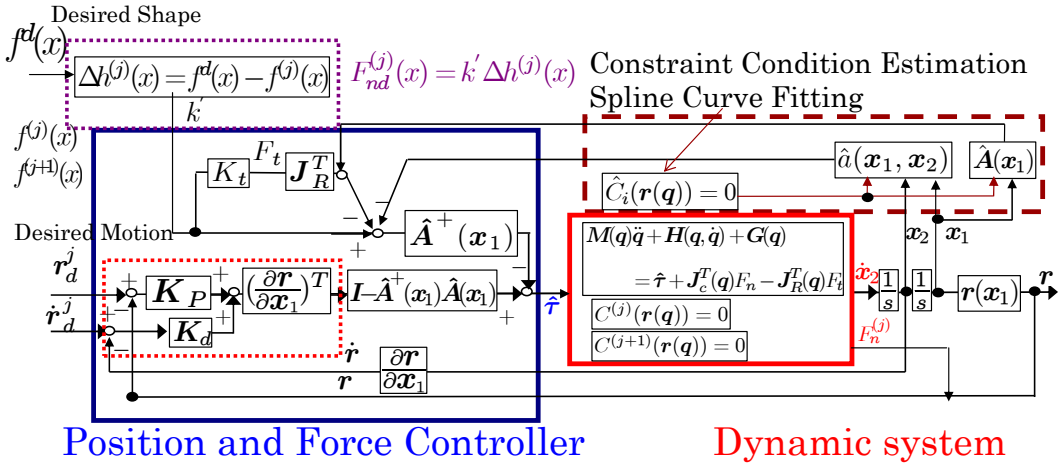

Fig. 2. Shape-grinding position / force control system

which is expressed as $\Delta h^{(j)}$ shown in Fig. 3 can be obtained easily.

$$\Delta h^{(j)}(x_i) = f^d(x)\big|_{x=x_i} - f^{(j)}(x)\big|_{x=x_i} \tag{14}$$

In this case, we can obviously find that the desired constrained force should not be a constant. It should be changed while $\Delta h^{(j)}$ changes. So we redefine the desired constrained force $F_{nd}^{(j)}$ as a function of $\Delta h^{(j)}$, shown as follows:

$$F_{nd}^{(j)}(x_i) = k^{'}\Delta h^{(j)}(x_i) \tag{15}$$

where $k^{'}$ is a constant, and $k^{'} = 1000$ in our experiment.

IV. Force and Position Controller

A. Controller using predicted constraint condition

Reviewing the dynamic equation(Eq. (3)) and constraint condition(Eq. (5)), it can be found that as $l > 1$, the number of input generalized forces is more than that of the constrained forces. From this point and Eq. (10) we can claim that there is some redundancy of constrained force between the input torque $\boldsymbol{\tau}$, and the constrained force F_n. This condition is much similar to the kinematical redundancy of redundant manipulator. Based on the above argument and assuming that, the parameters of the Eq. (10) are known and its state variables could be measured, and $a(\boldsymbol{x}_1, \boldsymbol{x}_2)$ and $\boldsymbol{A}(\boldsymbol{x}_1)$ could be calculated correctly, which means that the constraint condition $C = 0$ is prescribed. As a result, a control law is derived and can be expressed as

$$\boldsymbol{\tau} = -\boldsymbol{A}^{+}(\boldsymbol{x}_1)\Big\{F_{nd} - a(\boldsymbol{x}_1, \boldsymbol{x}_2) - \boldsymbol{A}(\boldsymbol{x}_1)\boldsymbol{J}_R^T F_t\Big\} + (\mathbf{I} - \boldsymbol{A}^{+}(\boldsymbol{x}_1)\boldsymbol{A}(\boldsymbol{x}_1))\boldsymbol{k}, \tag{16}$$

where $\mathbf{I}$ is a $l \times l$ identity matrix, F_{nd} is the desired constrained forces, $\boldsymbol{A}(\boldsymbol{x}_1)$ is defined in Eq. (10) and $\boldsymbol{A}^{+}(\boldsymbol{x}_1)$ is the pseudoinverse matrix of it, $a(\boldsymbol{x}_1, \boldsymbol{x}_2)$ is also defined in Eq. (10) and $\boldsymbol{k}$ is an arbitrary vector which is defined as

$$\boldsymbol{k} = \tilde{\boldsymbol{J}}_r^{\,T}(\boldsymbol{q})\Big\{\boldsymbol{K}_p(\boldsymbol{r}_d - \boldsymbol{r}) + \boldsymbol{K}_d(\dot{\boldsymbol{r}}_d - \dot{\boldsymbol{r}})\Big\}, \tag{17}$$

where $\boldsymbol{K}_p$ and $\boldsymbol{K}_d$ are gain matrices for position and the velocity control by the redundant degree of freedom of $\boldsymbol{A}(\boldsymbol{x}_1)$, $\boldsymbol{r}_d(\boldsymbol{q})$ is the desired position vector of the end-effector along the constrained surface and $\boldsymbol{r}(\boldsymbol{q})$ is the real position vector of it. Eq. (17) describes the 2-link rigid manipulator's arm compliance, we have to set $\boldsymbol{K}_p$ and $\boldsymbol{K}_d$ with a reasonable value, otherwise high-frequency response of position error will appear. The controller presented by Eq. (16) and Eq. (17) assumes that the constraint condition $C = 0$ be known precisely even though the grinding operation is a task to change the constraint condition. This looks like to be a contradiction, so we need to observe time-varying constraint conditions in real time by using grinding tip as a touch sensor.

The time-varying condition is estimated as an approximate constrained function by position of the manipulator hand, which is based on the estimated constrained surface location. The estimated condition is denoted by $\hat{C} = 0$(in this paper, "$\wedge$" means the situation of unknown constraint condition). Hence, $a(\boldsymbol{x}_1, \boldsymbol{x}_2)$ and $\boldsymbol{A}(\boldsymbol{x}_1)$ including $\partial\hat{C}/\partial\boldsymbol{q}$ and $\partial/\partial\boldsymbol{q}(\partial\hat{C}/\partial\boldsymbol{q})$ are changed to $\hat{a}(\boldsymbol{x}_1, \boldsymbol{x}_2)$ and $\hat{\boldsymbol{A}}(\boldsymbol{x}_1)$ as shown in Eq. (19), Eq. (20). They were used in the later simulations of the unknown constrained condition. As a result, a controller based on the estimated constrained condition is given as

$$\hat{\boldsymbol{\tau}} = -\hat{\boldsymbol{A}}^{+}(\boldsymbol{x}_1)\Big\{F_{nd} - \hat{a}(\boldsymbol{x}_1, \boldsymbol{x}_2) - \hat{\boldsymbol{A}}(\boldsymbol{x}_1)\boldsymbol{J}_R^T F_t\Big\} + (\mathbf{I} - \hat{\boldsymbol{A}}^{+}(\boldsymbol{x}_1)\hat{\boldsymbol{A}}(\boldsymbol{x}_1))\boldsymbol{k}, \tag{18}$$

$$m_c{}^{-1}\Big\| \frac{\partial\hat{C}}{\partial\boldsymbol{r}} \Big\|\{-[\frac{\partial}{\partial\boldsymbol{q}}(\frac{\partial\hat{C}}{\partial\boldsymbol{q}})\dot{\boldsymbol{q}}]\dot{\boldsymbol{q}} + (\frac{\partial\hat{C}}{\partial\boldsymbol{q}})\boldsymbol{M}^{-1}(\boldsymbol{h} + \boldsymbol{g})\} \triangleq \hat{a}(\boldsymbol{x}_1, \boldsymbol{x}_2) \tag{19}$$

$$m_c{}^{-1}\Big\| \frac{\partial\hat{C}}{\partial\boldsymbol{r}} \Big\|\{(\frac{\partial\hat{C}}{\partial\boldsymbol{q}})\boldsymbol{M}^{-1}\} \triangleq \hat{\boldsymbol{A}}(\boldsymbol{x}_1) \tag{20}$$

Figure 2 illustrates a control system constructed according to the above control law that consists of a position feedback

control loop and a force feedfoward control. It can be found from Eq. (10) and Eq. (18) that the constrained force always equals to the desired one explicitly if the estimated constraint condition equals to the real one, i.e., $C = \hat{C}$ and $F_t = 0$. This is based on the fact that force transmission is an instant process. In the next section, we will introduce a prediction method which is used to get $\hat{C}$ in current time.

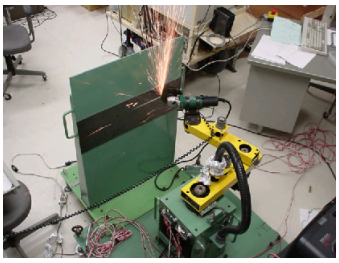

Fig. 4. The experiment when the constraint is known

for force control, then it happens that $\boldsymbol{A}(\boldsymbol{q})(\partial C/\partial \boldsymbol{q})^T/\parallel \partial C/\partial \boldsymbol{r} \parallel = \mathbf{I}$(identical matrix).

B. On-line Estimation of Constraint

As it is stated in former section, we had done the grinding experiment when working surface is flat and known, and now curve shape-grinding is proposed to be solved in our research. But how to predict the unknown constraint surface is the nodus and key point. Here, an unknown constrained condition is estimated as following,

Assumptions

1. The end point position of the manipulator during performing the grinding task can be surely measured and updated.
2. The grinding task is defined in $x - y$ plane.
3. When beginning to work, the initial condition of the end-effector is known and it has touched the work object.
4. The chipped and changed constraint condition can be approximated by connections of minute sections.

1) On-line estimation method: Some relations between position value and time value are written here, in this section, you'd better remember these relations because it will help you understand the concept of "on-line estimation method".

$$x_{i-1} = x(t_{i-1}) = x(t_0 + (i-1)\Delta t), \tag{21}$$

$$x_i = x(t_i) = x(t_0 + i\Delta t), \tag{22}$$

$$x_{i+1} = x(t_{i+1}) = x(t_0 + (i+1)\Delta t). \tag{23}$$

Before on-line estimation method is introduced, let's take

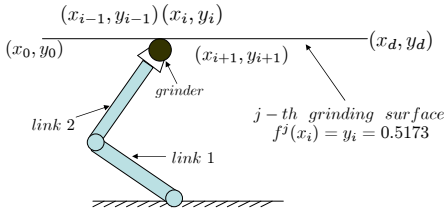

Fig. 5. Situation of known constraint surface model

a look at the situation of known flat constraint surface. For example, just like the grinding surface shown in Fig. 5, the expression of this surface is straight linear equation

$$f^j(x_i) = y_i = 0.5173(i = 0, 1, 2, 3...n), \tag{24}$$

and point (x_i, y_i) is the current position of grinding robot's end-effector. As a result, points before (x_i, y_i) have been already ground by grinder when $t <= t_0 + i\Delta t$. In the next moment, when time $t_{i+1} = t_0 + (i+1)\Delta t$, constraint condition

$$C^j_{i+1} = y - f^j(x_i) = 0 \tag{25}$$

can be used for calculation of deriving torque $\boldsymbol{\tau}$. And also, grinder will move to next point (x_{i+1}, y_{i+1}) with no hesitation driven by the input torque $\boldsymbol{\tau}$. By "no hesitation", I mean on this known surface, grinder has no where to go but point (x_{i+1}, y_{i+1}), since this whole grinding surface $f^j(x_i) = y_i = 0.5173(i = 0, 1, 2, 3...n)$ is determined obviously.

However, we all know that the grinding surface on work-piece after ground will turn into some kind of irregular shape that no mathematic equation can express. what should we do to obtain the future constraint condition C^j_{i+1} if the grinding surface is unknown? Like the situation shown in Fig. 6, the grinding surface is not a simple straight line or some curve line which can be defined and expressed by some certain curve equation, after current time $t_i = t_0 + i\Delta t$, where should the grinder go? Grinding robot has no idea since input torque $\boldsymbol{\tau}$ can not be derived without constraint condition C^j_{i+1}.

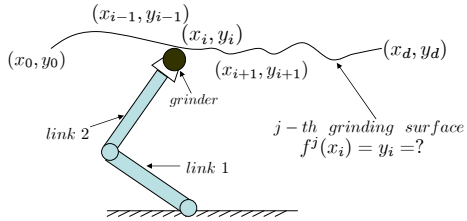

Fig. 6. On-line estimation model

To solve this problem, we consider that some kind of on-line estimation function should be utilized to imitate the unknown grinding surface, in order to obtain an unknown constraint condition $\hat{C^j_{i+1}}$, which can be used to calculate the input torque $\hat{\boldsymbol{\tau}}$.

Therefore, now let's take a look at Fig. 6, in current time $t_i = t_0 + i\Delta t$, end-effector of grinding robot is at position (x_i, y_i), so far, point (x_{i-1}, y_{i-1}) and point (x_i, y_i) have become known because they were just ground by the grinder in the moment $t_{i-1} = t_0 + (i-1)\Delta t$ and $t_i = t_0 + (i)\Delta t$ and the information of point (x_{i-1}, y_{i-1}) and (x_i, y_i) can be derived through the position of robot's end-effector. Now build an estimation function going through these two points, for example, a quadratic spline function

$$f^j_i(x_i) = f_{spline}(x_i) = y_i = \alpha_i(x - x_{i-1})^2 +$$

$$\beta_i(x - x_{i-1}) + \gamma_i$$

$$x \in [x_{i-1}, x_i](i = 0, 1, 2, 3...n), \tag{26}$$

we can figure out the coefficients α_i, β_i and γ_i uniquely according to the information of points (x_{i-1}, y_{i-1}), (x_i, y_i) and derivation at point (x_i, y_i) as follows.

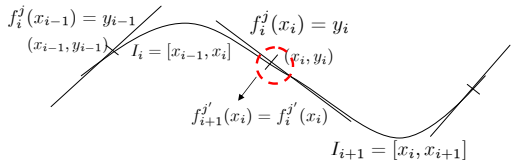

Fig. 7. Fitting by quadratic spline curve

Firstly, let $f_i^j(x_i)$ satisfy the following conditions shown in Fig. 7.

(A)Go through two ends of the interval

$$y_{i-1} = f_i^j(x_{i-1}) \tag{27}$$

$$y_i = f_i^j(x_i) \tag{28}$$

(B)First-order differential of the spline polynomials are equal at the end-point of adjoined function.

$$\frac{df_{i+1}^j(x)}{dx}\Big|_{x=x_i} = \frac{df_i^j(x)}{dx}\Big|_{x=x_i} f_{i+1}^{j'}(x_i) = f_i^{j'}(x_i) \tag{29}$$

Inputting (26) into (27), (28) and (29), we can obtain:

$$\gamma_i = y_{i-1}, (i = 1, 2, \cdots, n) \tag{30}$$

$$\beta_{i+1} = 2u_i - \beta_i, (i = 1, 2, \cdots, n-1) \tag{31}$$

$$\alpha_i = \frac{\beta_{i+1} - \beta_i}{2h_i}, (i = 1, 2, \cdots, n-1) \tag{32}$$

Where, $h_i = x_i - x_{i-1}$, $u_i = \frac{y_i - y_{i-1}}{h_i}$. From the above-mentioned result, the constrained conditional expression $\hat{\boldsymbol{C}}_{i+1}^j$ can be updated step by step.

Make an expansion of the interval between point (x_{i-1}, y_{i-1}) and point (x_{i+1}, y_{i+1}) on the grinding surface which is shown in Fig. 8, we can see the first half of grinding surface before the current position - point (x_i, y_i) is shown by black line, which means this part has been already ground, and second half after piont (x_i, y_i) is shown by break point line, which means this part has not been ground yet. Now let's pay our attention on the interval between point (x_i, y_i) and point (x_{i+1}, y_{i+1}), which means this part has been estimated by quadratic spline function. With the estimation function the next point (x_{i+1}, y_{i+1}) can easily be found to be known, and then this point can be the position where grinder should go in the next moment when $t_{i+1} = t_0 + (i+1)\Delta t$, At the same time, this imitative function can be used as the on-line estimation function to obtain the unknown constraint condition

$$\hat{C}_{i+1}^j = y - f_i^j(x) = y - [\alpha_i(x - x_{i-1})^2 + \beta_i(x - x_{i-1})$$

$$+\gamma_i] = 0, \ (x_i \le x \le x_{i+1}) \tag{33}$$

during the period when grinder goes from point (x_i, y_i) to point (x_{i+1}, y_{i+1}), which means in this unknown interval

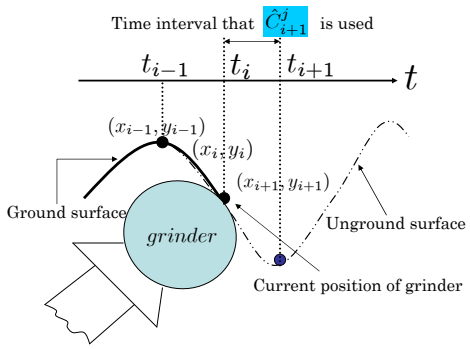

Fig. 8. The expansion of interval between point (x_{i-1}, y_{i-1}) and point (x_{i+1}, y_{i+1}) on the on-line estimation model

on the grinding surface, the future unground part (x_i, y_i) to (x_{i+1}, y_{i+1}) can be ground by this on-line estimation method based on the information obtained from already ground part (x_{i-1}, y_{i-1}) to (x_i, y_i). So, in the situation of unknown constraint surface, using this on-line estimation method point to point, the problem for grinding robot that it doesn't know where it should go in future time can be solved theoretically.

V. Experiment

A. Experiment purpose and devices

In this section, we will introduce a curve surface shape-grinding experiment on an iron work-piece with this proposed position/force control method. During this experiment, constraint condition $\hat{C}_{i+1}^j$ which has been explained before is always changing because of the changing constraint working surface. Based on the previous simulation result[19], we choose Quadratic spline function to estimate the changing constraint surface and build the constraint condition $\hat{C}_{i+1}^j$. Fig. 3 shows the experiment's grinding task. In Fig. 3, we can find that the desired surface is known(it can be determined by us, here we use Eqn. 34 to be this desired surface)

$$f^d(x_i) = 0.5173 + 0.015\cos(5\pi x_i + \frac{\pi}{2})[m]$$

$$(0.0m \le x_i \le 0.2m) \tag{34}$$

and also the initial flat surface is known(Eqn. 35)

$$f^1(x_i) = 0.5173[m] \qquad (0.0m \le x_i \le 0.2m) \tag{35}$$

TABLE I
Parameters of Grinding Robot

	link 1	link 2
mass of link [kg]	$m_1 = 12.28$	$m_2 = 7.64$
length of link [m]	$l_1 = 0.3$	$l_2 = 0.5$
gravity center of link [m]	$a_1 = 0.24$	$a_2 = 0.25$
general coordinates [rad]	q_1	q_2
input torque [N]	$\hat{\tau}_1$	$\hat{\tau}_2$

Here we notice that although the initial constraint surface $f^1(x_i)$ and desired constraint surface $f^d(x_i)$ are known already, those functions $f^j(x_i)$ who can express the constraint working sufaces between $f^1(x_i)$ and $f^d(x_i)$ are unknown.

Therefore, we utilize the quadratic spline function to estimate them.

$$f^j(x_i) = f_{spline}(x_i) \qquad (0.0m \leq x_i \leq 0.2m) \tag{36}$$

The initial constraint surface to be ground is defined as $(x, y) = (0.0, 0.5173) \sim (0.2, 0.5173)$[m] in time 5.0[s], and the desired velocity along the surface is 0.04[m/s]. The desired force, F_{nd}, is set as

$$F^j_{nd}(x_i) = k^{'} \Delta h^j(x_i)[N] \qquad (k = 1000) \tag{37}$$

$\Delta h(x_i)$ indicates the distance between the current surface and desired surface, shown in Fig. 3.

$$\Delta h^j(x_i) = f^d(x_i) - f^j(x_i) = f^d(x_i) - f_{spline}(x_i) \tag{38}$$

Grinding robot's parameters are listed in Table. I, and there are two motors(produced by YASKAWA Ltd.) mounted on those two links used in torque control mode whose output torque can be designated by the input voltage to the amplifier to each motor, where motor of AC$(400[W], 200[V])$ drives link 1, motor of AC $(200[W], 200[V])$ drives link 2. Link 1's Torque/Voltage is 0.42[Nm/V], link 2's Torque/Voltage is 0.21[Nm/V].

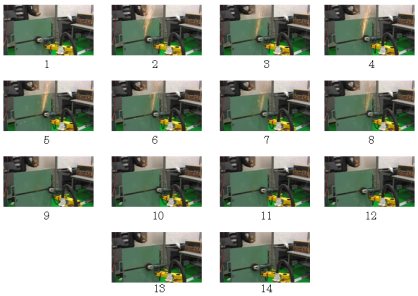

Fig. 9. Performance of shape-grinding experiment

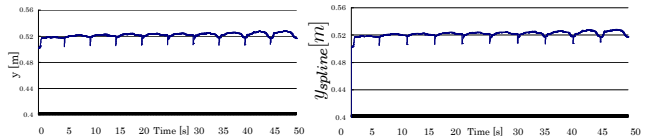

Fig. 10. Comparison of actual and estimated shape during 10 times' experiment

B. Experiment results

In this section, we will show and introduce the final 10 times' shape-grinding experiment result. It takes 5 seconds for each time, so in total there are 50 seconds had been used to do this experiment. Fig. 9 shows the performance of this grinding robot during 10 times' shape grinding experiment. The left figure of Fig. 10 shows the 10 times' working surfaces ground by robot's grinder, which is mounted on the tip of grinding robot's hand, and meanwhile the right one in Fig. 10 has recorded the surfaces' functions which are estimated by quadratic spline function. Compare these two figures, we can tell that the estimated trajectory has almost the same value of the real ground surfaces.

Desired shape of this experiment has been recorded and shown in Fig. 11. Here we set the desired shape as a curve with a deepest position $150mm$, and the work-piece used in this shape-grind experiment is an iron board, which is very hard to grind, so if we want to grind the whole curve shape, experiment should be done by almost 300 times. But to verify the effectiveness of this force-sensorless position/force control method, 10 times' successful experiment will do if we can obtain an obvious small curve shape after grinding work. Therefore, although this very deep desired curve shape has been set, it is just used as a generator of desired grinding force F_{nd} through Eqn. 37.

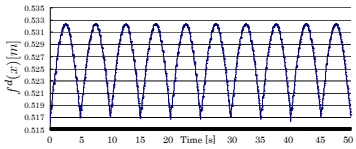

Fig. 11. Desired shape of grinding experiment

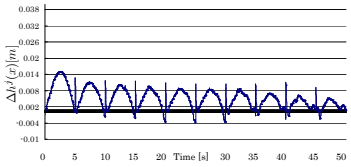

Fig. 12. Distance between current grinding surface and desired surface during 10 times' grinding experiment

The distance between current grinding surface and desired surface during 10 times' grinding experiment, expressed by $\Delta h^j(x_i)$ is shown in Fig. 12. The desired grinding force F_{nd} calculated by Eqn. 37 is shown by the left figure in Fig. 13. From this figure, we can see that the desired grinding force's value is bigger than $10N$ sometimes, and smaller than $0N$ at the beginning point, so to make sure that stable touch between grinder and work-piece can be obtained in order to do this grinding experiment safely, in the controller system we set a threshold to select those safe and useful value to be utilized, which is shown by the right figure in Fig. 13.

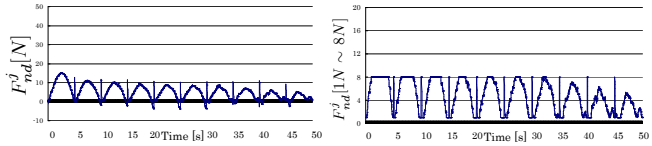

Fig. 13. Desired constraint force F_{nd} decided by Δh in 10 times' experiment

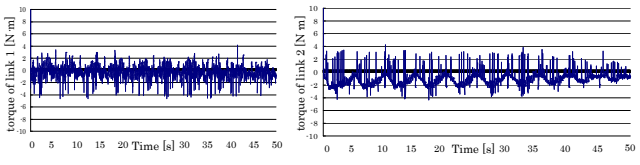

Fig. 14. Change of torque $\hat{\tau}_{1,2}$ during 10 times' experiment

The input torques $\hat{\tau}_{1,2}$ calculated with the unknown constraint condition $\hat{C}$ are shown in Fig. 14. Since the unknown constraint condition $\hat{C}$ is built by quadratic spline estimation method, the viberation of quadratic spline function's coefficient A_i(shown in Fig. 15) is affecting the input torques $\hat{\tau}_{1,2}$ during the whole experiment time. Fig. 16 shows the real

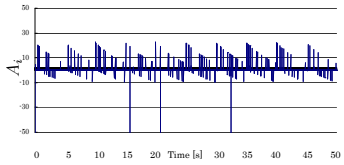

Fig. 15. Change of spline function's coefficient A_i

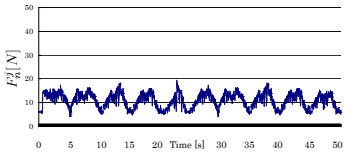

Fig. 16. Real constraint force F_n measured by force sensor

constraint grinding force measured by a force sensor. After 10 times grinding, we can see the iron board has been ground a lot in Fig. 17, and also a small curve shape has been ground out although the iron board is very hard to grind. The deepest position on this small curve is about $0.5mm$, so according to this grinding speed, we believe that if the grinding robot to be told to do this shape-grinding experiment more than 50 times, we can get a much bigger curve shape with a more than $2mm$'s deepest position.

Through this 10 times' continuous shape-grinding experiment result, the effectiveness and feasibility of force-sensorless position/force control method can be verified.

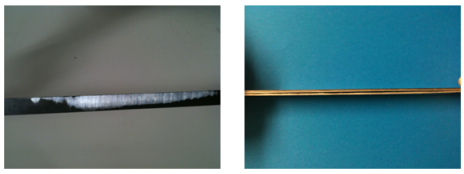

Fig. 17. The appearance of ground work-piece

VI. Conclusions

Constraint dynamic equation of manipulator is expressed as an explicit function of the manipulator's state and inputs. Manipulator's hand tip is used as a position sensor, to supply those necessary information for this proposed force and position control methodology. Hence, the system is controlled without any force or torque sensor. The control law presented is constructed by using the dynamical redundancy of constraint systems. The controller designed by this control law can be used for simultaneous force and position control.

Simulation has been done to verify the effectiveness of four constraint condition estimation methods[19], and the quadratic spline function is chosen to estimate the unknown constraint surface in shape-grinding experiment. 10 times' shape-grinding experimnet has been done based on the proposed force and position control law without force or torque sensor. Although there are still some problems left in the grinding robot, but the force-sensorless position/force control method and continuous shape-grinding practicability has been verified through the experiment result. In the future, we believe that this force-sensorless position/force control method can be utilized in many robotic control fields.

References

[1] M.H.Raibert and J.J.Craig: Hybrid Position/Force Control of Manipulators, Trans. of the ASME, J. of Dynamic Systems, Measurement and Control, Vol.102, pp.126-133, June, 1981.

[2] S. Arimoto, Mechanics and Control of Robot(in Japanese), Asakura Publishing Co., Ltd., Tokyo, Japan, 1990.

[3] T. Yoshikawa: Dynamic Hybrid Position/Force control of Robot Manipulators — Description of Hand Constraints and Calculation of Joint Driving Force, IEEE J. on Robotics and Automation, Vol.RA-3, No.5, pp.386-392, 1987.

[4] L. Whitcomb, S. Arimoto, T. Naniwa and F. Osaki, Experiments in Adaptive Model-Based Force Control, IEEE Control Systems Society, Vol.16, No.1, pp.49-57, 1996.

[5] S. Arimoto: Joint-Space Orthogonalization and Passivity for Physical Interpretations of Dextrous Robot Motions under Geometric Constrains, Int. J. of Robust and Nonlinear Control, Vol.5, pp.269-284, 1995.

[6] D.Wang and N.H. McClamroch: Position and Force Control for Constrained Manipulator Motion: Lyapunov's Direct Approach, IEEE Trans. Robotics and Automation, Vol.9, pp.308-313, 1993.

[7] Z. X. Peng and N. Adachi: Position and Force Control of Manipulators without Using Force Sensors(in Japanese), Trans. of JSME(C), Vol.57, No.537, pp.1625-1630, 1991.

[8] Jaydeep. Roy and Louis L. Whitcomb: Adaptive Force Control of Position/Velocity Controlled Robots: Theory and Experiment, IEEE Transactions on Robotics and Automation, Vol.18, No.2, April, 2002.

[9] Suguru Arimoto, Control Theory of Non-Linear Mechanical Systems, Oxford University Press, 1996.

[10] B. Siciliano, L. Villani, Robot Force Control, Kluwer Academic Publishers, U.K., 1999.

[11] C. Natale, Interaction Control of Robot Manipulators, Springer Tracts in Advanced Robotics, Germany, 2003.

[12] N. Hogan: Impedance control: An approach to manipulation: Part 1-Theory, J.Dynamic Syst., Measurement Contr., Vol.107, pp.1-7, Mar, 1985.

[13] B. Siciliano and L. Villani: A passivity-based approach to force regulation and motion control of robot manipulators, Automatica, Vol.32, No.3,pp.443-447, Mar, 1996.

[14] L. Villani, C.C. de Wit and B. Brogliato: An exponentially stable adaptive control for force and position tracking of robot manipulators, IEEE Trans. Automat. Contr., Vol44, pp.778-802, Apr, 1999.

[15] J. De Schutter and H.Van Brussel: Compliant robot motion 2. A control approach based on external control loops, Int. J. Robot. Res., Vol.7, No.4, pp.18-33, Aug, 1988.

[16] Hooshang Hemami and Bostwick F. Wyman: Modeling and Control of Constrained Dynamic Systems with Application to Biped Locomotion in the Frontal Plane, IEEE Trans. on Automatic Control, Vol.AC-24, No.4, pp.526-535, 1979.

[17] Takeshi Ikeda, Mamoru Minami, Position/Force Control of a Manipulator by Using an Algebraic Relation and Evaluations by Experiments, The 2003 IEEE/ASME Int. Conf. on Advanced Intelligent Mechatronics (AIM2003), Proceeding CD-ROM paper No.159, 503-508, 2003

[18] Takeshi Ikeda and Mamoru Minami: Research of Grinding Robot without Force Sensor by Using Algebraic Equation(in Japanese), Transactions of the Japan Society of Mechanical Engineers(C), Vol.71, No.702, pp.270-277, 2005.

[19] Mamoru Minami, Weiwei Xu, Shape-grinding by Direct Position / Force Control with On-line Constraint Estimation, 2008 IEEE/RSJ International Conference on Intelligent Robots and Systems, Acropolis Convention Center, Nice, France, Sept, 22-26, 2008. pp. 943-948